Full Paper

Effect of the Alkyl Chain Length Incorporated into Donor Part on the Optoelectronic Properties of the Carbazole Based Dyes: Theoretical Study

Souad El Mzioui[a], Si Mohamed Bouzzine*[a,b], Mohammed Bouachrine[c], Mohamed Naciri Bennani[d], Mohamed Hamidi[a]

[a]*Equipe d'Electrochimie et Environnement, Faculté des Sciences et Techniques, Université Moulay Ismaîl, B.P 509 Boutalamine, Errachidia, Maroc.*
[b]*Centre Régional des Métiers d'Education et de Formation, B.P 8, Draâ Tafilalet, Errachidia, Maroc.*
[c]*Ecole Supérieure de Technologie, Université Moulay Ismail Meknès, Maroc.*
[d]*Equipe du Matériaux et Catalyse Appliqués, Département de Chimie, Faculté des Sciences, Université Moulay Ismail, B.P. 11201-Zitoune, Meknès, Maroc.*

Abstract: In this paper, we report a theoretical study using density functional theory (DFT) and time-dependent (TD-DFT) for R-D-π-A systems with various alkyl chains (R). Results show that the LUMO of the dye lies above the semiconductor conduction band, promoting the injection of electrons; the lower HOMO level promotes dye regeneration. The incorporation of methyl chain (CH_3) has a significant reduction in the gap energy, improved red-shift absorption spectrum and increase the molar extinction coefficient at the maximum absorption wavelength compared to D. While, the increase in alkyl chain length from C_2H_5 to C_6H_{13} present a relatively reduce of gap energies, low effect on the wavelength (438 nm) and converged excitation energies.

Keywords: R-D-π-A structure; effect of alkyl chain length; electronics properties

1. INTRODUCTION

Dye Sensitized Solar Cells (DSSCs) have been widely investigated since the first report by O'Regan and Grätzel in 1991 [1], due to their easy and low cost fabrication procedure [2], environment friendliness, greater structural flexibility, higher molar extinction coefficient, and reasonably good power conversion efficiency [3-4]. These characteristics make them a possible competitor to traditional inorganic silicon for photovoltaic cells. Ru-complex dyes are unsuitable for cost-effective and environment friendly photovoltaic systems because they contain the noble metal ruthenium; expensive resources and the difficult purification process of metal limit their widespread application in DSSCs [2].

Most organic dyes are composed of a push-pull Donor-π-Acceptor (D-π-A) structure due to its effective better intramolecular charge transfer characteristics [5]. Organic dyes having carbazole and its derivatives [6] and triphenylamine [7-9] as the donor moiety have been reported to show remarkable efficiency in DSSC devices. The carbazole donor has been usually used for building block in push-pull D-π-A structure for the organic sensitizers and optical materials because of their strong donating ability [17-18]. Thiophene and its derivatives are choosing as the best candidates for the π-conjugated systems, in particular bithiophene. They exhibits the best charge transport properties, due to reduced band gap energy and better photoconversion of electric current [19]. Cyano-acrylic acid is the most commonly used as acceptor moiety due to the existence of the cyanide group that has a strong electron accepting ability [20]. We use π-bridge spacers to link the donor and acceptor. The π-bridge help to relay the electron density and facilitate charge separation upon excitation. Therefore, engineering of organic sensitizer with a reduced tendency toward aggregation is paramount. A successful approach was introduced by incorporating some alkyl chains into the organic framework, which not only suppresses aggregate

---

formation but also enhances the molar extinction coefficient of the organic sensitizer [21]

In this study, we have designed a series of R-D-π-A type of organic dyes with thiophene-carbazole as the electron donor (D), bithiophene as the π-conjugated bridge and cyanoacrylic acid as the electron acceptor (A). Keeping all other units fixed and varying the alkyl group (R) from CH_3 to C_6H_{13}, we elucidated the effect of the different alkyl chain on the geometric, electronic, and optical properties of such dye for their use as sensitizers in solar cells.

2. MATERIAL AND METHODS

The ground state of the dye optimized with Density Functional Theory (DFT) using the B3LYP functional [22] and 6-31G (d,p) basis set with the Gaussian 09 [23]. The structures are minima on the potential energy surface and their harmonic vibrational frequencies are positive of all compounds. Moreover, the excited state calculations were carried using Time-Dependent (TD-DFT) with the same hybrid functional and basis set to simulate the UV-Vis absorption spectra in chloroform solvent by using the polarizable continuum model of solvation (CPCM) [24]. The energy levels of the molecular orbital and the isodensity plot were extrapolated in isolated state to show the electronic density distribution that used for description of optic and electronic properties of donor-π-acceptor sensitizers.

3. RESULTS AND DISCUSSION

In order to gain insight of the effect of different alkyl chains on the geometrical, electronic and optical properties of organic dyes, we have studied, in this work, a dye based on carbazole donor and Bithiophene Bridge. The dye namely D was substituted by different C_nH_{2n+1} alkyl chains (with n =

0 to 6) on the donor part (Scheme 1) and the theoretical study was optimized using DFT and TD-DFT methods.
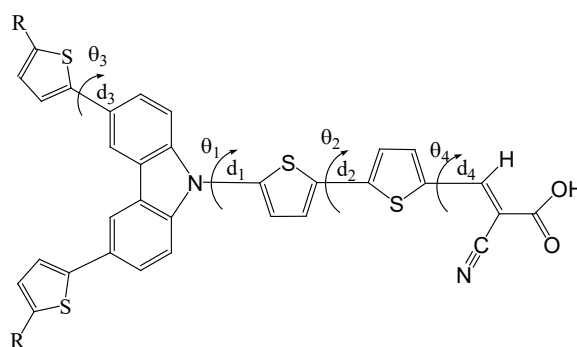
Scheme 1. Structures of D substituted by different alkyl chain (R) or R= C_nH_{2n+1} (n=0 to 6).

3.1. Geometrical properties

The geometrical values of all studied dyes are shown in Table 1. The calculated ground-state bond lengths for all studied dyes are about 1.39; 1.44; 1.46 and 1.42 Å for d_1, d_2, d_3 and d_4 respectively. These distances are in range of 1.38–1.44 Å showing significant C=C character, which improved the intramolecular charge transfer [25]. The dihedral angles values (Table 1) shown that the optimized geometry of all sensitizers is not totally planar, in particularly, θ_1 and θ_3, which show an important decrease inside plan for the dyes substituted by the methyl chain CH_3 . Although, for the same dye D-CH_3, θ_2 and θ_4 present a significant decrease in out-plan. Moreover the substitution by C_nH_{2n+1} (n=2 to 6) showed a little variation in the dihedral angle. These results mean that the incorporation of the methyl chain into thiophene donor unit induced an important distortion of the dihedral angle. However, the increase in alkyl chain length from C_2H_5 to C_6H_{13} has a little variation on the dihedral angles.

Table 1. Bond distances (d_1, d_2, d_3, d_4) and dihedral angles (θ_1, θ_2, θ_3, θ_4) of D substituted by C_nH_{2n+1} alkyl chain calculated by B3LYP/6-31G(d,p) in isolated state.

R	d_1 (Å)	d_2 (Å)	d_3 (Å)	d_4 (Å)	θ_1 (°)	θ_2 (°)	θ_3 (°)	θ_4 (°)
H	1.393	1.443	1.469	1.426	56.11	179.09	29.80	179.95
CH_3	1.392	1.443	1.468	1.425	55.05	178.84	28.77	179.95
C_2H_5	1.392	1.443	1.468	1.425	55.11	178.35	28.80	179.93
C_3H_7	1.392	1.443	1.468	1.425	55.01	178.00	29.01	179.93
C_4H_9	1.392	1.443	1.468	1.425	54.69	178.39	29.24	179.94
C_5H_{11}	1.392	1.443	1.468	1.425	54.74	177.45	29.42	179.91
C_6H_{13}	1.392	1.443	1.468	1.425	54.39	177.64	29.50	179.90

330

Orbital: Electron. J. Chem. 9 (5): 329-336, 2017

3.2. Electronic properties

Table 2 represents the electronic properties (including the HOMO, LUMO and Gap energies values) of the dye D substituted with different chain alkyl and compared with the corresponding experimental results. The calculated HOMO, LUMO and gap energy levels of D and $D-C_6H_{13}$ are in quite good agreement with the experimental analogues compounds DWH1 and DWH2 obtained by J-F Huang and all [26], Indicating the validation of the functional (B3LYP) and the method (DFT).

The $D-CH_3$ dye (2.37 eV) with incorporation of the methyl chain shows a reduction in the gap energy of 0.11 eV compared with D (2.48 eV). Whereas when the length of the alkyl chain was varied, HOMOs and LUMOs energy values display a very little variation that giving the Gap energy values about 2.36eV. These results indicate that the incorporation of methyl chain CH_3 results in a small Reduction of the gap energy that improves the electronic properties of the dye. Moreover, the dye substituted by the alkyl chain CH_3 to C_6H_{13} showed similar electronic properties, which can lead to similar overall efficiencies. These results are also obtained by Y-H Lee et al [29], they found that there is no variation in the gap energy (2.82 eV) when the alkyl chain was increased from C_4H_9 to $C_{12}H_{25}$.

Table 2. Energy values of HOMOs, LUMOs, and E_{gap} (eV) of D substituted by C_nH_{2n+1} (n=0 to 6) alkyl chain calculated B3LYP/6-31G(d,p) in isolated state.

R	E_{HOMO}	E_{HOMO}*	E_{LUMO}	E_{LUMO}*	E_{gap}	E_{gap}*
H	−5.38	−5.65	−2.90	−3.19	2.48	2.46
CH_3	−5.24	-	−2.87	-	2.37	-
C_2H_5	−5.22	-	−2.86	-	2.36	-
C_3H_7	−5.22	-	−2.86	-	2.36	-
C_4H_9	−5.21	-	−2.86	-	2.36	-
C_5H_{11}	−5.21	-	−2.85	-	2.36	-
C_6H_{13}	−5.21	−5.66	−2.85	−3.23	2.36	2.43

*: Experimental data [26]

3.3. Absorption spectra

The UV-visible absorption spectra reported for all studied dyes in chloroform solvent are revealed in Figure 1. The summarized data including wavelength absorption, oscillator strength, light harvesting efficiency and molar extinction coefficient are shown in Table 3. These results show that all studied dyes exhibits three principal bands. The peaks positioned at lower energy region appearing at about 578-604 nm are attributed to the intramolecular charge transfer (ICT) between the thiophene-carbazole donor and the cyanoacrylic acid. The intense peaks at about 432-438 nm can be assigned to the localized π-π* transition with an important oscillator strength of 0.9-1. Whereas the peak at 300 nm has a flow form, it is unclear and presents a very small oscillator strength (0.06-0,1).

The band appeared at 432 nm for D and that at 438 nm for $D-C_6H_{13}$ are in good agreement with experimental data λ_{max}(D namely DWH1 in his work)=434 nm and λ_{max}(D-C_6H_{13} namely DWH2 in his work)=436 nm [26], implying that the TD-B3LYP

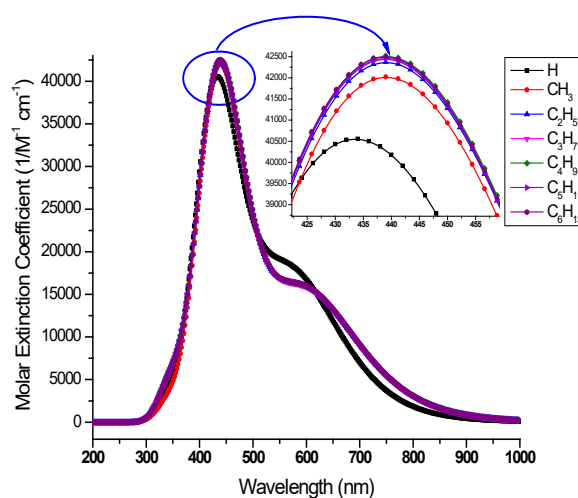functional is valid for reproducing the absorption bands.

Figure 1. Absorption spectra of D substituted by different alkyl chains in chloroform.

$D-CH_3$ peak at 438.27 is red-shifted by 6.28 nm compared to the D peak at 432 nm, which indicate

331

Orbital: Electron. J. Chem. 9 (5): 329-336, 2017

that the introduction of methyl chain on the thiophene donor is very important for improved the red-shift absorption spectrum and also increase the molar extinction coefficient (Table 3) at the maximum absorption wavelength compared to D. While the variation of the alkyl chain length from CH_3 to C_6H_{13} has a low effect on the wavelength (438 nm), the value of Light Harvesting Efficiency (LHE≈0.9), (table 3 and figure 1). Q-Y Yu and al [27] also obtain these results. The latter found that the compound C6 (λ_{max}=503 nm) with the C_6H_{13} alkyl chain and the compound C9 (λ_{max}=504 nm) with presented the nearby wavelength absorption. The difference between the molar extinction coefficient of D-CH_3 and D-C_6H_{13} at the maximum absorption is also small (about 479 M^{-1} cm^{-1}) that is comparable with the experimental difference between C_4 and C_{12} (about 923 M^{-1} cm^{-1}) [29], which indicate the marginally effect obtained with C_6H_{13} compared to CH_3.

The UV-visible absorption data showed that there is an important decrease in the excitation energies (eV) from dye D to D-CH_3. The excitation energies almost converged by varying from dye D1-CH_3 to C_6H_{13} (Figure 2). These lower and converged excitation energies of dyes D-C_nH_{2n+1} (n=2 to 6) may be responsible for showing higher and similar efficiencies over dyes D and D-CH_3. So, we can use just the methyl alkyl chain instead of the longest, in the theoretical investigation, in order to minimize the calculation times.

Therefore, the incorporation of long alkyl chain in organic sensitizers can be used experimentally to decrease the undesirable formation of dye aggregates on the surface of the semiconductor and to decrease recombination processes between TiO_2 electrons and electrolyte species. The long alkyl chain is also used to enhance the stability of sensitizers, increase the solubilization of the dyes structure and improve the lifetimes of DSSC devices [30].

Table 3. Wavelength absorption (**λ**), oscillator strength (f), the light harvesting efficiency (LHE) and molar extinction coefficient (ε) of D substituted by C_nH_{2n+1} alkyl chain calculated by TD-B3LYP/6-31G(d,p) in chloroform solvent.

R	E (eV)	λ (nm)	λ* (nm)	f	LHE	ε (M-1, cm-1)	Major contribution
	2143	578.60	-	0.411	0.611	18148	H→L (99%
H	2.870	432.00	434	0.979	0.895	40556	H-2→L (99%)
	3.602	344.22	-	0.056	0.122	-	H→L+1 (16%), H→L+2 (77%)
	2.055	603.24	-	0.366	0.569	15901	H→L (99%)
CH_3	2.829	438.27	-	1.021	0.905	42025	H-2→L (98%)
	3.538	350.45	-	0.060	0.129	-	H→L+1 (10%), H→L+2 (83%)
	2.050	604.89	-	0.364	0.567	15800	H→L (99%)
C_2H_5	2.827	438.62	-	1.028	0.906	42374	H-2→L (98%)
	3.535	350.73	-	0.124	0.249		H-4→L (34%), H→L+1 (10%), H→L+2 (52%)
	2.050	604.91	-	0.363	0.566	15741	H→L (99%)
C_3H_7	2.827	438.58	-	1.030	0.907	42473	H-2→L (98%)
	3.533	350.89	-	0.119	0.240		H-4→L (91%)
	2.049	605.15	-	0.365	0.568	15822	H→L (99%)
C_4H_9	2.827	438.63	-	1.031	0.907	42519	H-2→L (98%)
	3.532	351.01	-	0.121	0.243		H-4→L (91%)
	2.051	604.56	-	0.366	0.569	15888	H→L (99%)
C_5H_{11}	2.828	438.48	-	1.030	0.907	42451	H-2→L (98%)
	3.532	351.06	-	0.116	0.234		H-4→L (93%)
	2.051	604.62	-	0.366	0.569	15884	H→L (99%)
C_6H_{13}	2.828	438.43	436	1.031	0.907	42504	H-2→L (98%)
	3.532	351.05	-	0.116	0.234		H-4→L (93%)

H : HOMO and L : LUMO.   *: Experimental data [26]

332

Orbital: Electron. J. Chem. 9 (5): 329-336, 2017

3.4. Molecular orbital calculations

We plotted the electron spatial distribution of the HOMO-2, HOMO, and LUMO molecular orbitals involved in the electron transitions of the studied dyes in Figure 4. The HOMO-2 and HOMO orbitals display anti-bonding character between two adjacent fragments and bonding character within each unit. While the LUMO orbital exhibits bonding character between the two adjacent fragments and anti-bonding character within each unit.

The electron densities of the HOMO levels in all the studied dyes are mainly originated from the π-orbitals of the donor consisting by carbazole and thiophene. The HOMO-2 electron densities are localized in the bithiophene bridge and cyanoacrylic acid acceptor. While the LUMO levels are largely dominating contributions from the π^*-orbitals of the cyanoacrylic acid and the nearby π-linkers, which facilitate the electron charge transfer from the donor to acceptor. The contribution of electronic transition from HOMO to LUMO is ~99% for all dyes. The HOMO eigenvalues of all the dyes (Figure 3) were lower than the redox potential (-4.8 eV) of the I^-/I^{3-} redox couple [31], which facilitates effective dye regeneration from its oxidized state. More the LUMO is above the conduction band TiO_2 semiconductor (-4.00 eV) [32], so the electron injection from the excited state of the dye to the conduction band of TiO_2 would be facilitated. Depend on figure 3, there was little variation in the LUMO and LUMO energies with increasing the alkyl chain length from CH_3 to C_6H_{13} and the energy values almost converged. Such electronic distribution of the HOMOs and LUMOs indicates that HOMO−LUMO excitation moves the electron from the donor part to the cyanoacrylic acid through the π-linker groups, ensuring efficient charge separation and electron injection.
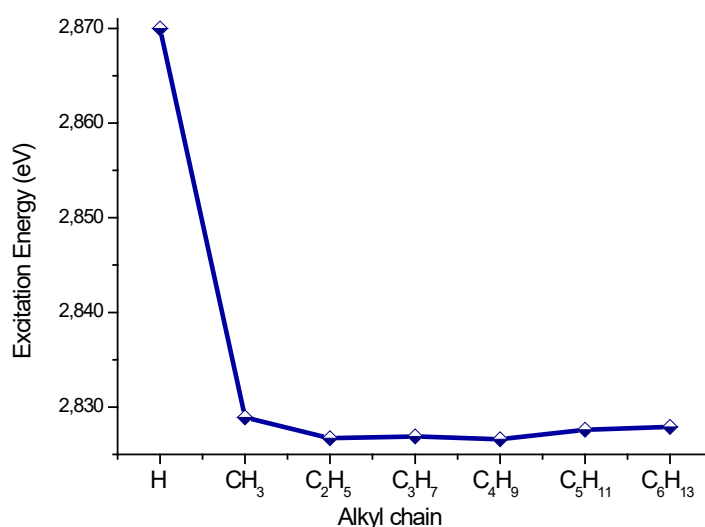

Figure 2. Variation of excitation energy with the increase of alkyl chain length.
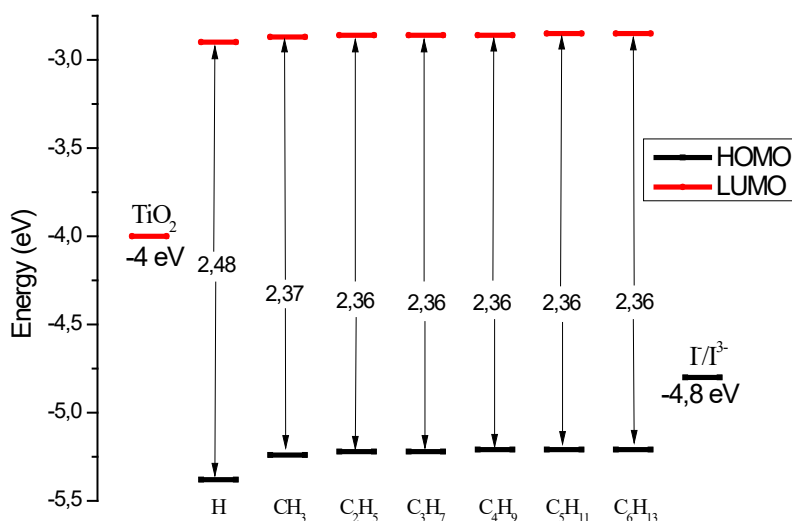

Figure 3. HOMO, LUMO and Gap energy level of D-C_nH_{2n+1} (n=0 to 6).

333
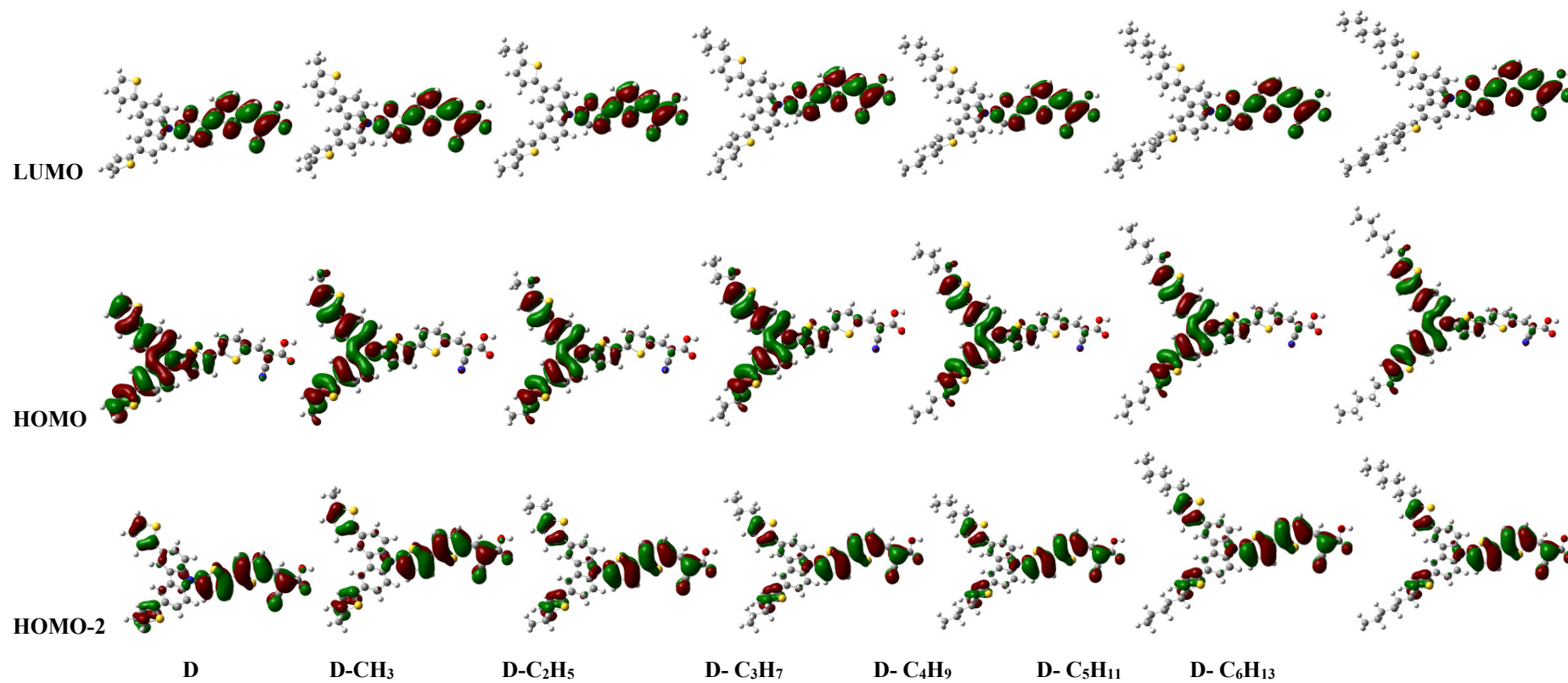
Orbital: Electron. J. Chem. 9 (5): 329-336, 2017

Figure 4. Visualization of frontier molecular orbitals (FMOs) of all dyes.

4. CONCLUSION

The theoretical calculation obtained by the DFT/B3LYP/6-31G(d,p) for the ground state optimization and TD-DFT/B3LYP/6-31G(d,p) for the excited state have shown that the introduction of CH_3 methyl chain has an important reduction in the gap energy, improved red-shift absorption spectrum and increase the molar extinction coefficient at the maximum absorption wavelength. However, increase in alkyl chain length from C_2H_5 to C_6H_{13} present a relatively reduce of gap energies, has a low effect on the wavelength (438 nm), has almost converged excitation energies. Therefore, the long alkyl chain can be used experimentally to decrease the undesirable formation of dye aggregates on the surface of the semiconductor and to decrease recombination processes between TiO_2 electrons and electrolyte species.

5. ACKNOWLEDGMENTS

6. REFERENCES AND NOTES

[1] O'Regan, B.; Grätzel, M. *Nature* **1991**, *353*, 737. [CrossRef]

[2] Mishra, A.; Fischer, M. K. R.; Bauerle, P. *Angew. Chem. Int. Ed.* 2009, 48, 2474. [CrossRef]

[3] Hagfeldt, A.; Boschloo, G.; Sun, L. C.; Kloo, L.; Pettersson, H. *Chem. Rev.* **2010**, *110*, 6595. [CrossRef]

[4] Goncalves, L. M.; Bermudez, V. D.; Ribeiro, H. A.; Mendes, A. M. *Energy Environ. Sci.* **2008**, *1*, 655. [CrossRef]

[5] Cai, S. ; Tian, G. ; Li, X. ; Su, J. ; Tian, H. *J. Mater. Chem. A* 2013, 1, 11295. [CrossRef]

[6] Koumura, N.; Wang, Z. S.; Mori, S.; Miyashita, M.; Suzuki, E.; Hara, K. *J. Am. Chem. Soc.* **2006**, *128*, 14256. [CrossRef]

[7] Hwang, S.; Lee, J. H.; Park, C.; Lee,'H.; Kim, C.; Park, C.; Lee, M. H.; Lee, W.; Park, J.; Kim, K.; Park, N. G.; Kim, C. *Chem. Commun.* **2007**, *46*, 4887. [CrossRef]

[8] Liang, M.; Chen, J. *Chem. Soc. Rev.* **2013**, *42*, 3453. [CrossRef]

[9] Cai, L.; Moehl, T.; Moon, S. J.; Decoppet, J. D.; Humphry-Baker, R.; Xue, Z.; Bin, L.; Zakeeruddin, S. M.; Grätzel, M. *Org. Lett.* **2014**, *16*, 106. [CrossRef]

[10] Wang, Z. S.; Cui, Y.; Dan-Oh, Y.; Kasada, C.; Shinpo, A.; Hara, K. *J. Phys. Chem. C* **2007**, *111*, 7224. [CrossRef]

[11] Wang, Z. S.; Cui, Y.; Dan-Oh, Y.; Kasada, C.; Shinpo, A.; Hara, K. *J. Phys. Chem. C* **2008**, *112*, 17011. [CrossRef]

[12] Liu, B.; Wang, R.; Mi, W. J.; Lia, X. Y.; Yu, H. T. *J. Mater. Chem.* **2012**, *22*, 15379. [CrossRef]

[13] Liu, J.; Yang, X. D.; Islam, A.; Numata, Y.; Zhang, S. F.; Salim, N. T.; Chen, H.; Han, L. *J. Mater. Chem. A* **2013**, *1,* 10889. [CrossRef]

[14] Kim, J. Y.; Kim, Y. H.; Kim, Y. S. *Curr. Appl. Phys.* **2011**, *11*, S117. [CrossRef]

[15] Liu, B.; Wu, W.; Li, X.; Li, L.; Guo, S.; Wei, X.; Zhu, W.; Liu, Q. *Chem. Chem. Phys.* **2011**, *13*, 8985. [CrossRef]

[16] Liu, B.; Li, W.; Wang, B.; Li, X.; Liu, Q.; Naruta, Y.; Zhu, W. *J. Power Sources* **2013**, *234*, 139. [CrossRef]

[17] Wang, S.; Wang, H.; Gu, J. C.; Tang, H.; Zhao, J. *Dyes Pigm.* **2014**, *109*, 96. [CrossRef]

[18] Zhao, Z.; Xu, X.; Wang, H.; Lu, P.; Yu, G.; Liu, Y. *J. Org. Chem.* **2008**, *73*, 594. [CrossRef]

[19] Li, T.; Gao, J.; Cui, Y.; Zhong, C.; Ye, Q.; Han, L. *J. Photochem. Photobiol., A* **2015**, *303*, 91. [CrossRef]

[20] Raju, T. B.; Vaghasiya, J. V.; Afroz, M. A.; Soni, S. S.; Iyer, P. K. *Org. Elect.* **2016**, *39*, 371. [CrossRef]

[21] (a) Yu, Q. Y.; Liao, J. Y.; Zhou, S. M.; Shen, Y.; Liu, J. M.; Kuang, D. B. *J. Phys. Chem. C* **2011**, *115*, 22002. [CrossRef] (b) Koumura, N.; Wang, Z. S.; Mori, S.; Miyashita, M.; Suzuki, E.; Hara, K. *J. Am. Chem. Soc.* **2006**, *128*, 14256e7. [CrossRef]

[22] Becke, A. D. *J. Chem. Phys.* **1993**, *98*, 5648. [CrossRef]

[23] Frisch, M. J.; Trucks, G. W.; Schlegel, H. B.; Scuseria, G. E.; Robb, M. A.; Cheeseman, J. R.; Scalmani, G.; Barone, V.; Mennucci, B.; Petersson, G. A.; Nakatsuji, H.; Caricato, M.; Li, X.; Hratchian, H. P.; Izmaylov, A. F.; Bloino, J.; Zheng, G.; Sonnenberg, J. L.; Hada, M.; Ehara, M.; Toyota, K.; Fukuda, R.; Hasegawa, J.; Ishida, M.; Nakajima, T.; Honda, Y.; Kitao, O.; Nakai, H.; Vreven, T.; Montgomery, Jr., J. A.; Peralta, J. E.; Ogliaro, F.; Bearpark, M.; Heyd, J. J.; Brothers, E.; Kudin, K. N.; Staroverov, V. N.; Kobayashi, R.; Normand, J.; Raghavachari, K.; Rendell, A.; Burant, J. C.; Iyengar, S. S.; Tomasi, J.; Cossi, M.; Rega, N.; Millam, N. J.; Klene, M.; Knox, J. E.; Cross, J. B.; Bakken, V.; Adamo, C.; Jaramillo, J.; Gomperts, R.; Stratmann, R. E.; Yazyev, O.; Austin, A. J.; Cammi, R.; Pomelli, C.; Ochterski, J. W.; Martin, R. L.; Morokuma, K.; Zakrzewski, V. G.; Voth, G. A.; Salvador, P.; Dannenberg, J. J.; Dapprich, S.; Daniels, A. D.; Farkas, Ö.; Foresman, J. B.; Ortiz, J. V.; Cioslowski, J.; Fox, D. J. Gaussian 09, Revision A.1, Gaussian, Inc.: Wallingford, CT, 2009.

[24] Grisorio, R.; De Marco, L.; Giannuzzi, R.; Gigli, G.; Suranna G. P. *Dyes and Pigments* **2016**, *131*, 282. [CrossRef]

[25] Fitri, A.; Benjelloun, A. T.; Benzakour, M.; Mcharfi, M.; Hamidi, M.; Bouachrine, M. *Spectrochim. Acta, Part A* **2014**, *132*, 232. [CrossRef]

[26] Huang, J. F.; Liu, J. M.; Tan, L. L.; Chen, Y. F.; Shen, Y.; Xiao, L. M.; Kuang, D. B.; Su, C. Y. *Dyes and Pigments* **2015**, *114*, 18. [CrossRef]

[27] Yu, Q. Y.; Liao, J. Y.; Zhou, S. M.; Shen, Y.; Liu, J. M.; Kuang, D. B.; Su, C. Y. *J. Phys. Chem. C* **2011**, *115*,

335

Orbital: Electron. J. Chem. 9 (5): 329-336, 2017

22002. [CrossRef]

[28] Baldoli, C.; Bertuolo, S.; Licandro, E.; Viglianti, L.; Mussini, P.; Marotta, G.; Salvatori, P.; De Angelis, F.; Manca, P.; Manfredi, N.; Abbotto, A. *Dyes and Pigments* **2015***, 121*, 351. [CrossRef]

[29] Lee, Y. H.; Chitumalla, R. K.; Jang, B. Y.; Jang, J.; Thogiti, S.; Kim, J. H. *Dyes and Pigments 2016*, *133*, 161. [CrtossRef]

[30] Joly, D.; Godfroy, M.; Pellejà, L.; Kervella, Y.; Maldivi, P.; Narbey, S.; Oswald, F.; Palomares, E.; Demadrille, R. *J. Mater. Chem. A* **2017**, *5*, 6122. [CrossRef]

[31] Zhang, J.; Li, H. B.; Sun, S. L.; Geng, Y.; Wu, Y.; Su, Z. M. *J. Mater. Chem.* **2012**, *22*, 568. [CrossRef]

[32] Preat, J.; Jacquemin, D.; Michaux, C.; Perpète*,* E. A. *Chem. Phys*. **2010**, *376*, 56. [CrossRef]

336

Orbital: Electron. J. Chem. 9 (5): 329-336, 2017